# CHAPTER 2
# DILUTED MAGNETIC SEMICONDUCTORS – A REVIEW

## 2.1 Introduction

The first generation of spintronics devices were based on passive magnetoresistive sensors and memory elements using electrodes made from alloys of ferromagnetic 3d metals. Their development was later boosted by the discovery of giant magnetoresistance, in $(Fe/Cr)_n$ multilayers, and tunnelling magnetoresistance[1]. Next generation is expected to consist on active spin-based devices that will necessarily comprise the creation and manipulation of spin-polarized electrons in a host semiconductor[2,3]. In order to achieve an operational device, the electrons must be spin-polarized and their polarization largely preserved as they travel through the semiconductor material. The most obvious way for spin injection would be injecting from a FM metal in a metal/SC junction. This type of heterostructures have been extensively studied; however, it has been shown that it is difficult to preserve the electron spin across the interface, mainly due to the large mismatch in electrical conductivity between the two materials[4]. On the contrary, magnetic semiconductors should allow easier integrability with the existing semiconductor technology, and would be vital for signal amplification with highly spin-polarized carriers. Therefore, the design of materials combining both SC and FM properties turns to be crucial in the development of such devices and presents a serious materials physics challenge.

It was in this context that the concept of diluted magnetic semiconductor (DMS) emerged. DMSs are non-magnetic semiconductors doped with a few percent of magnetic elements, usually transition-metals (TM) (see figure 2.1), and are expected to be not only easily integrable with existing semiconductors but also highly spin-polarised. However, the discovery and understanding of such materials are proving to be a grand challenge in solid-state science. Indeed, one of the 125 critical unanswered scientific questions recently raised in a commemorative issue of Science magazine[5,6] asks, *"Is it possible to create magnetic semiconductors that work at room temperature?"*. The materials challenge is great because both magnetic and electronic doping is required, and the interaction between magnetic dopant spins and free carriers must be engineered to achieve thermally robust dopant spin-

carrier coupling[6].

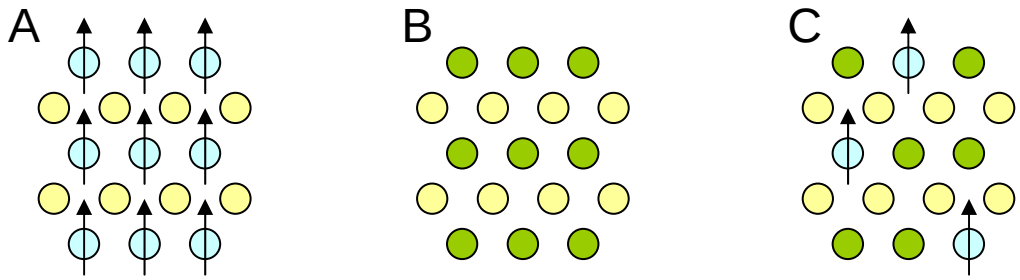


**Figure 2.1** Schematic showing (A) a magnetic semiconductor, (B) a non-magnetic semiconductor material, and (C) a diluted magnetic semiconductor (adapted from ref. 7).

Magnetism and semiconducting properties are known to coexist in some ferromagnetic semiconductors, such as europium chalcogenides and ferrimagnetic or ferromagnetic semiconducting spinels[7]. The first DMSs to be identified were II-VI semiconductor alloys like $Zn_{1-x}Mn_xTe$ and $Cd_{1-x}Mn_xTe$[8]. They were studied in the 1980s, presenting either spin glass behavior or weak ferromagnetism, with Curie temperatures ($T_c$) of only a few K[9] and, therefore, completely inadequate for applications requiring ferromagnetic order at room temperature (RT). More recently, the Mn-doped III–V semiconductors $In_{1-x}Mn_xAs$[10,11] and $Ga_{1-x}Mn_xAs$[12,13] showed ferromagnetism at higher temperature. A $T_c$ of 173 K was achieved in Mn-doped GaAs by using low temperature annealing techniques which is quite promising[14,15], although still too low for the envisaged RT applications.

In all these materials ferromagnetism has been proven to be carrier mediated, which enables the modification of magnetic behaviour through charge manipulation. This has motivated a continuous search for materials with even higher $T_c$ and carrier mediated ferromagnetism, and led to the conjecture that oxide-based DMS would be key materials in the development of spintronic devices. Indeed, it was pointed out that the capability of high electron doping and the rather heavy effective electron mass of oxide semiconductors could be quite efficient to realize high Curie temperatures[16]. Moreover, most of the foreseen oxide-based DMSs are wide band gap semiconductors (>3eV) which can add an optoelectronic dimension to the new generation of spintronic devices. In this context, the groundbreaking was the discovery of RT ferromagnetism in the $Co:TiO_2$ system by Matsumoto *et al.*[17,18], which has triggered a considerable number of investigations in other oxide-based DMS such as TM-doped ZnO[19], $SnO_2$[20], $Cu_2O$[21] and $In_{1.8}Sn_{0.2}O_3$[22]. Table 2.1

summarises the magnetic moments and $T_c$ values reported in literature for thin films of these oxide-based DMSs.

**Table 2.1** Some reports on high $T_c$ oxide-based DMS (adapted from ref. 23).

| **Material** | **Doping (*x*)** | **Moment ($\mu_B$/3d ion)** | **$T_c$ (K)** |
|---|---|---|---|
| $TiO_2$ | Co, 1-2%<br>Co, 7%<br>V, 5%<br>Fe, 2% | 0.3<br>1.4<br>4.2<br>2.4 | > 300<br>650 - 700<br>> 400<br>> 300 |
| ZnO | Co, 10%<br>V, 15%<br>Mn, 2.2%<br>Fe, 5% - Cu, 1%<br>Ni, 0.9% | 2.0<br>0.5<br>0.16<br>0.75<br>0.06 | 280 - 300<br>> 350<br>> 300<br>550<br>> 300 |
| $SnO_2$ | Co, 5%<br>Fe, 5% | 7.5<br>1.8 | 650<br>610 |
| $Cu_2O$ | Co, 5% - Al, 0.5% | 0.2 | > 300 |
| $In_{1.8}Sn_{0.2}O_3$ | Mn, 5% | 0.8 | > 300 |

## 2.2 $TiO_2$ based DMSs – literature review

Among the oxide-based DMS materials investigated, Co:$TiO_2$ system seems to be the most consistently reported *n*-type semiconductor material to present ferromagnetic order far above RT ($T_c$ > 650 K)[24], although a consensus on the origin of the ferromagnetic coupling has not yet been achieved, as will be later discussed, which in some cases is probably due to the presence of Co clusters. This review describes the general properties of the titanium dioxide ($TiO_2$), the experimental status on the preparation of thin films of Co-doped $TiO_2$, and the mechanisms by which their ferromagnetic order might be promoted.

### 2.2.1 The titanium dioxide

Titanium dioxide is a versatile wide band gap oxide semiconductor that has been extensively used in optical components and in heterogeneous photo-oxidation catalysis for environmental cleanup issues[25-27]. Moreover, it has a great potential application as non-linear optical material[28], in dye-sensitized solar cells[29], in gas sensors[30] and in dynamic random access memories[31]. $TiO_2$ occurs in three distinct polymorph forms: rutile, anatase

and brookite. Their crystal structures are summarized in table 2.2.

**Table 2.2** Structural properties of the different $TiO_2$ polymorphs[32].

| Phase | System | Space Group | Lattice constants (nm) | | | Density (kg m$^{-3}$) |
|---|---|---|---|---|---|---|
| | | | ***a*** | ***b*** | ***c*** | |
| Rutile | Tetragonal | $D_{4h}^{14} - P4_2/mnm$ | 0.4584 | 0.4584 | 0.2953 | 4240 |
| Anatase | Tetragonal | $D_{4h}^{19} - I4_1/amd$ | 0.3782 | 0.3782 | 0.9502 | 3820 |
| Brookite | Rhombohedral | $D_{2h}^{15} - Pbca$ | 0.5436 | 0.9166 | 0.5135 | 4170 |

Among the three natural $TiO_2$ structures, rutile is the most stable and also the most compact one. In contrast, anatase is the most open structure being almost 10% less dense than rutile (see table 2.2). The remarkable density difference between anatase and rutile plays an important role in differentiating the properties of the two structures but, in the same time, it is less dramatic than expected. Parameters reflecting the nature of the bonding mechanism, such as the atom coordination and average bond length, are very similar in the two structures. The extra volume in anatase corresponds to empty regions and affects only those properties that are averaged on the whole cell such as the compressibility or the dielectric constant.

The different structures of titanium dioxide are commonly described as constituted by a different arrangement of the same building block: a $TiO_6$ group where the titanium atom (the cation) sits in the center and is surrounded by six oxygen atoms (the anions) situated at the corners of a distorted octahedron. Each structure is characterized by a particular distortion of the octahedra and different assembly patterns. In all natural modifications of $TiO_2$, the octahedra are distorted in such a way that two oxygen atoms (apical atoms) are slightly more distant from the central titanium atom than the remaining four (equatorial atoms).

The unit cell of rutile and anatase are shown in figure 2.2. In both structures there are six atoms per unit cell and all atoms of the same element are equivalent by symmetry. Anatase is a body centred structure so that the represented conventional cell contains two unit cells (12 atoms). The titanium atoms, and hence the octahedra, are arranged in such a way that each oxygen is at the same time an equatorial atom for one titanium, and an apical one for

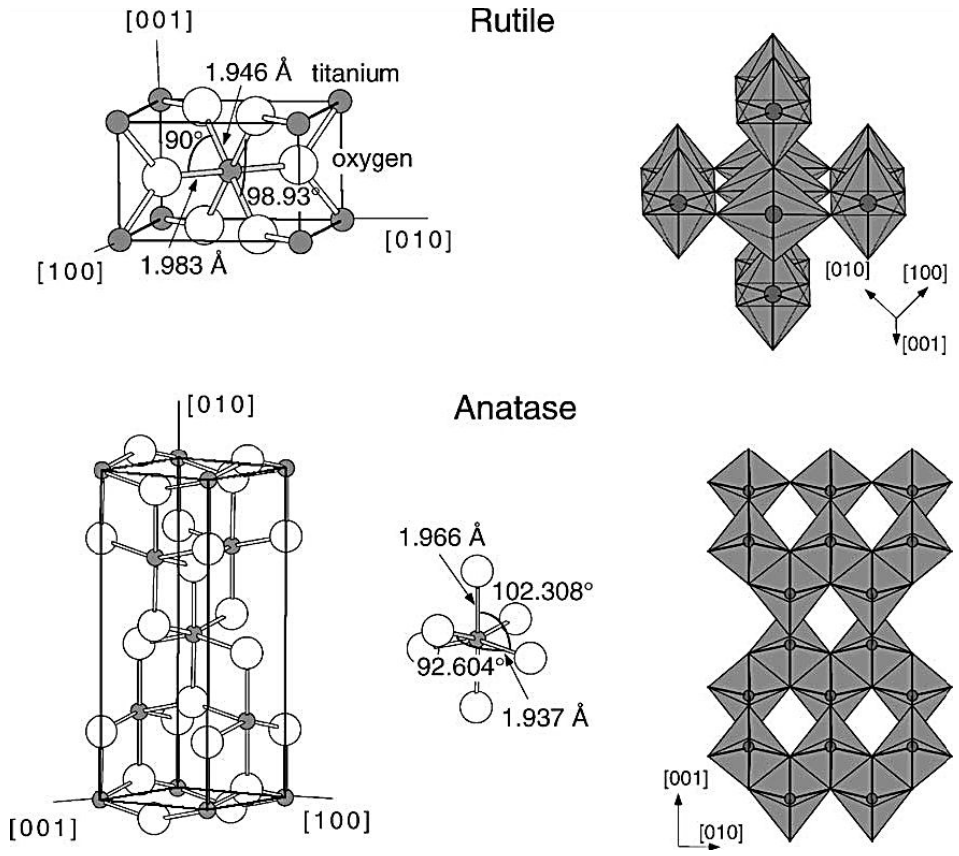


**Figure 2.2** Bulk structure of rutile and anatase. The tetragonal bulk unit cell of rutile has the dimensions, a = b = 4.587 Å, c = 2.953 Å, and the one of anatase a = b = 3.782 Å, c = 9.502 Å. In both structures, slightly distorted octahedra are the basic buildings units. The bond lengths and angles of the octahedrally coordinated Ti atoms are indicated and the stacking of the octahedra in both structures is shown on the right hand side (adapted from ref. 32).

the other titanium atom in the same unit cell. Neighbouring octahedra are sharing edges and corners with each other. Two and four edges of each octahedron are shared in rutile and anatase, respectively. The basic octahedra are distorted in such a way that each shared edge is shortened, the other edges being correspondingly elongated. In rutile, the bridge bond is connecting two equatorial oxygen atoms. The octahedral are hence forming vertical linear chains. The octahedra belonging to adjacent chains are connected only through one corner: an oxygen atom which is, at the same time, apical and equatorial for the two touching octahedra. Contiguous chains are related by the four-fold symmetry of the space group: 90º rotation around the principal tetragonal axis followed by a fractional translation bringing the central titanium atom to its equivalent location. In anatase, the octahedra are arranged in order to share a diagonal edge between an apical and an equatorial atom. Octahedra are hence forming zig-zag chains orthogonal to the

crystallographic axis. There are two sets of chains orthogonal to each other and connected through a common octahedron.

The energy band structure of $TiO_2$ rutile phase has been extensively studied. Both experimental results and theoretical calculations suggest that high quality rutile crystals have a direct forbidden gap of 3.03 eV, which is almost degenerate with an indirect allowed transition of 3.05 eV (406 nm)[33,34]. Due to the weak strength of the direct forbidden transition, the indirect allowed transition dominates in the optical absorption just above the absorption edge[35]. The fundamental absorption edge of bulk $TiO_2$ anatase phase was reported to be 3.2 eV (387 nm)[36], also assigned to an indirect transition. However, it should be noticed that band gap energies close to the values referred above were also experimentally deduced assuming direct transitions in the case of $TiO_2$ nanopowders, for both rutile and anatase forms[37]. Only recently an indirect band gap of 3.4 eV was measured for the $TiO_2$ brookite phase[38]. Electronic properties of both the rutile and anatase $TiO_2$ phases are summarized in table 2.3, according to the review by Fukumura *et al.*[39].

**Table 2.3** Electronic properties of both rutile and anatase $TiO_2$ phases; $\rho$, $n$ and $\mu$ stand for resistivity, carrier density and mobility, respectively[39].

| **Material** | $\rho$ **(Ω cm)** | $n$ **(cm$^{-3}$)** | $\mu$ **(cm$^2$ V$^{-1}$ s$^{-1}$)** |
|---|---|---|---|
| Rutile | $3\times10^{-3}$ - $2\times10^{-1}$ | $10^{18}$ - $10^{21}$ | 0.05 - 0.2 |
| Anatase | $6\times10^{-2}$ - $8\times10^{-2}$ | $7\times10^{18}$ - $2\times10^{21}$ | 6 - 10 |

## 2.2.2 Growth and properties of Co-doped $TiO_2$ thin films

The earliest observation of RT ferromagnetism in the Co:$TiO_2$ system was reported by Matsumoto et al.[17], who synthesised anatase phase $Ti_{1-x}Co_xO_2$ films ($0 \leq x \leq 0.08$) on $LaAlO_3$(0001) and $SrTiO_3$(001) substrates by combinatorial laser molecular beam epitaxy using oxygen pressures in the range $10^{-6}$ – $10^{-5}$ mbar and substrate growth temperatures between 680 and 720ºC. A few months later, the same research group reported RT ferromagnetism in rutile phase $Ti_{1-x}Co_xO_2$ ($0 \leq x \leq 0.05$) thin films grown onto α-$Al_2O_3$ substrates, using the same deposition technique[18].

Since then, the synthesis of both anatase and rutile Co:$TiO_2$ ferromagnetic films have been achieved using several physical and chemical deposition techniques. Most of the films

have been grown using pulsed laser deposition (PLD)[40-45] but reactive co-sputtering[46], metal-organic chemical vapour deposition (MOCVD)[47], oxygen-plasma-assisted molecular beam epitaxy (OPA-MBE)[48-50], laser molecular beam epitaxy (LMBE)[51-53], and even sol-gel method[54] have also been employed. In addition, a range of growth conditions and various substrates have been explored. Anatase/rutile $TiO_2$ thin films can be prepared on different substrates such as α-$Al_2O_3$(1102)[18], $SrTiO_3$(001)[17,40,41,43,49,50], $LaAlO_3$(001) [17,40,43,49], Si(100)[46] and $SiO_2$/Si[47]. The substrate influences, and sometimes even determines the phase of $TiO_2$ that is formed. On $LaAlO_3$(001) only the anatase phase has been grown, independently of the growth method[17,40,49,51,55-60], which can be explained by the very small lattice misfit of −0.26 % between $LaAlO_3$(001) substrate and the $TiO_2$ anatase phase. The lattice mismatch between $TiO_2$ (001) anatase and $SrTiO_3$(001) substrate is −3.1% so, although the anatase phase was found in many investigations[17,40,48,55,61- 63], this is not always the case.

Anatase Co:$TiO_2$ films deposited on $SrTiO_3$ are (001) oriented as shown by S.R. Shinde *et al.*[40] and the low value ~ 0.3º of the full width at half-maximum (FWHM) of the rocking curve confirms their high crystalline quality. The substrate deposition temperature varies from one technique to the other − 700 ºC for PLD, 550 ºC in OPA-MBE[48] and 500 ºC in MOCVD[47], but the non-dependence of the (anatase) grown phase on the substrate temperature was confirmed by Chambers *et al.*[49].

In contrast, films grown on Si(100) and $Al_2O_3$(0001) always exhibit the rutile structure, unless buffer layers are grown in between the substrate and the $TiO_2$ thin film[64]. As will be seen in chapter 5, our results on growth onto sapphire show that this is not always the case – anatase and/or rutile growth also depends on the laser fluence and background pressure besides substrate type and growth temperature.

The quality of the Co-doped $TiO_2$ films depends strongly on the oxygen pressure during the deposition, as shown by Kim *et al.*[41]. Films grown at $P_{O_2} \geq 1.3\times10^{-5}$ mbar showed clear streaky RHEED patterns, which suggest two-dimensional layer-by-layer growth with very smooth surfaces. For the films grown at lower $P_{O_2}$ as the film growth progressed, the patterns turned into three-dimensional spotty patterns[41]. The rocking curve of the (004) peak for the film grown at $1.3\times10^{-5}$ mbar shows a FWHM of 0.66°, which is similar to those values reported by Murakami *et al.*[65]. As $P_{O_2}$ decreased down to $1.3\times10^{-7}$ mbar, the FWHM increased to 0.86°, indicating that films grown under the low $P_{O_2}$ show a wider

mosaic spread[41].

The Co distribution inside the $TiO_2$ matrix depends very much on the deposition conditions. Kim *et al.*[41] suggested that a possible factor influencing the Co distribution could be the presence of oxygen vacancies. They found an increasing tendency of Co to clustering with decreasing $P_{O_2}$. If a low $P_{O_2}$ is assumed during growth the number of oxygen vacancies in the sample increases, the formation of Co clusters beeing explained by the higher mobility of Co in the $TiO_2$ lattice. The diffusion of Co, at least up to $x = 0.1$, seems to be easily attainable in the $TiO_2$[48] although a value as high as $x = 0.12$ was reported[46]. On the other hand, Shinde *et al.*[40] reported limited solubility up to ~2% Co in PLD as-grown films and formation of Co clusters of size 20-50 nm, as well as a small content of Co incorporated into the remaining matrix. After being subjected to the high temperature annealing, these clusters were seen to dissolve in the $TiO_2$ matrix. In the case of thin films with greater Co concentration, i.e. 5%, Co clusters of about 150 nm were observed[48].

Furthermore, the Co distribution in the films was found to depend critically on the way in which the growth process was terminated. For instance, Chambers *et al.*[48] showed that for $Co_xTi_{1-x}O_2$ films grown by OPA-MBE onto $SrTiO_3$ substrates, stopping growth by simultaneously closing the metal source shutters, turning off the oxygen plasma, and pumping out the residual oxygen as the sample cooled, consistently produced films which were either stoichiometric or substoichiometric in Co, depending also on substrate temperature. In contrast, terminating the growth by closing the metal shutters and allowing the sample to cool in the oxygen plasma beam consistently resulted in significant Co segregation within the near surface region ($x$ as large as ~0.5). X-ray photoelectron spectroscopy depth profiles revealed that the Co concentration in such films decays exponentially with depth away from the surface, is essentially zero in the middle region of the film, and then increases slightly at the $Co_xTi_{1-x}O_2$ /$SrTiO_3$ interface.

The wide variety of Co-doped $TiO_2$ thin films produced have been characterized by X-ray diffraction (XRD) to determine the crystal structure, and often by conventional as well as high resolution transmission electron microscopy (HRTEM) to reveal the presence of defects such as dislocations and grain boundaries as well as the occurrence of precipitates and metallic Co particles. As the X-ray photoelectron spectroscopy (XPS) probes the electronic core state of an atom by knocking out an inner electron, this technique has been

used to identify the oxidation state and bonding environment of Co ions. X-ray absorption spectroscopy (XAS) probes the unoccupied electronic structure and the chemical environment of atoms in solids, and electron energy-loss spectroscopy (EELS) has been used to probe the electronic structure and to determine the oxidation state of Co in $TiO_2$. The magnetic properties of the films, in particular their saturation magnetization, have been investigated by superconducting quantum interference devices (SQUID) and vibrating sample magnetometry (VSM). Optical magnetic circular dichroism (MCD) as well as the anomalous Hall effect measurements have also been used to investigate the occurrence of intrinsic ferromagnetism.

Room temperature (RT) ferro- magnetism in Co-doped $TiO_2$ thin films was found to be independent of the substrate used in the deposition process, as clearly shown by different authors[7]. The SQUID data in references[7,17,46] all show Curie temperatures greater than 400 K. In particular, combining SQUID and VSM measurements, Shinde *et al.*[40] deduced a $T_c$ ~ 650 K for an annealed $Ti_{0.93}C_{0.07}O_{2-\delta}$ film (see figure 2.3), and a $T_c$ ~ 700 K for an as-grown $Ti_{0.99}C_{0.01}O_2$ film.

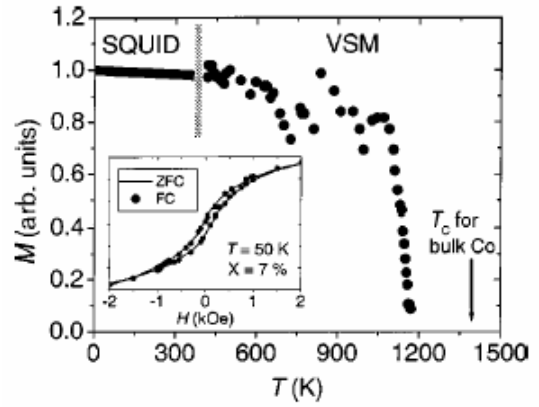


**Figure 2.3** The *M-T* data for a $Ti_{0.93}Co_{0.07}O_{2-\delta}$ film. The inset shows the hysteresis loops obtained under zero-field-cooling (ZFC) and field-cooling (FC) conditions (from ref. 40).

Saturation magnetization values ranging from 0.16 $\mu_B$/Co to as high as 2 $\mu_B$/Co have been reported for $Ti_{1-x}Co_xO_2$ thin films (table 2.4). Such a wide spread of magnetic moments has raised concerns about the intrinsic nature of the ferromagnetic properties of the Co:$TiO_2$ films, namely due to the possibility of existing cobalt secondary phases [41,43,51,67], heterogeneities or even contamination[68,69]. On the other hand, the presence of oxygen vacancies has been pointed out as a possible factor influencing the ferromagnetic behaviour of the films[51,68,72]; it has never been clearly shown whether it induces Co clustering and/or promotes magnetic ordering.

**Table 2.4** Saturation magnetization values per Co ion.

| Film composition | Substrate | $M_s$ ($\mu_B$/Co) | Ref. |
|---|---|---|---|
| $Co_{0.07}Ti_{0.93}O_2$ | $LaAlO_3$ | 0.32 | 17 |
| $Co_{0.05}Ti_{0.95}O_2$ | $\alpha$-$Al_2O_3$ | 1 | 18 |
| $Co_{0.07}Ti_{0.93}O_2$ | $SrTiO_3$, $LaAlO_3$ | 1.4 | 40 |
| $Co_{0.04}Ti_{0.96}O_2$ | SrTiO3 | 1.7 | 41 |
| $Co_{0.07}Ti_{0.93}O_2$ | $LaAlO_3$, SrTiO3 | 1.7±0.4 | 43 |
| $Co_xTi_{1-x}O_2$ (> 6%) | Si, quartz | 0.94 | 46 |
| $Co_{0.07}Ti_{0.93}O_2$ | $LaAlO_3$ | 1.2 | 50 |
| Co:$TiO_2$ | Si | 0.31 | 55 |
| Co:$TiO_2$ | $LaAlO_3$ | 0.23 | 55 |
| Co:$TiO_2$ | $SrTiO_3$ | 0.16 | 55 |
| Co:TiO2 | $LaAlO_3$ | 2.0 | 66 |

While the mechanism for ferromagnetism has not yet been definitively clarified, these controversial results have prompted many speculations that the growth conditions of the samples and/or the subsequent annealing conditions can be one of the important factors that determine their ferromagnetic behaviour.

For instance, N.J. Seong *et al.*[47] showed that at Co contents $x \leq 0.05$, the Co-doped $TiO_2$ thin films display an homogeneous structure without any clusters and exhibit pure ferromagnetic properties that can be attributed to the $Co_xTi_{1-x}O_2$ phase; in contrast, for $x > 0.05$, clusters having soft magnetic (SM) properties are formed in the homogeneous $Co_xTi_{1-x}O_2$ matrix and the overall magnetic behaviour depends on the ferromagnetic properties of both $Co_xTi_{1-x}O_2$ and Co clusters (Fig. 2.4). Furthermore, they showed that in the case $x > 0.05$ the saturation magnetization increases abruptly and the coercive field markedly decreases, confirming that the magnetic properties of the $Co_xTi_{1-x}O_2$ thin films depend on the Co doping level. These results suggest that the growth conditions, in particular the oxygen pressure, play an important role in the formation of Co clusters and/or the Co:$TiO_2$ phase and thus lead to a wide range of magnetic moments from 0.3 to 1.7 $\mu_B$/Co. This was confirmed by Kim *et al.*[41] who studied the dependence of magnetic moment *per* Co atom as a function of the oxygen pressure. They showed that most of the films deposited at $P_{O_2} \leq 3\times10^{-5}$ Torr (~ $4\times10^{-5}$ mbar) had saturation magnetization values close to that of bulk cobalt (1.7 $\mu_B$/Co). For the film grown at $P_{O_2} = 1.3\times10^{-7}$ mbar the magnetization does not decrease much with temperature. This dependence of the magnetic properties of the $Ti_{0.96}Co_{0.04}O_2$ thin films was explained in terms of the formation of Co

nanoclusters. The oxygen vacancies in the anatase Co-doped $TiO_2$ films grown on $SrTiO_3$ at low oxygen pressure help the Co ions to diffuse resulting in the formation of the nanoclusters and, as the number of Co clusters increases, the saturation magnetization will become larger. In films with similar composition and structure, $Co_xTi_{1-x}O_2$ ($x$ = 0.05), Chambers *et al.*[50] found a remanence and a coercivity of 0.24 $\mu_B$/Co and 125 Oe, respectively.

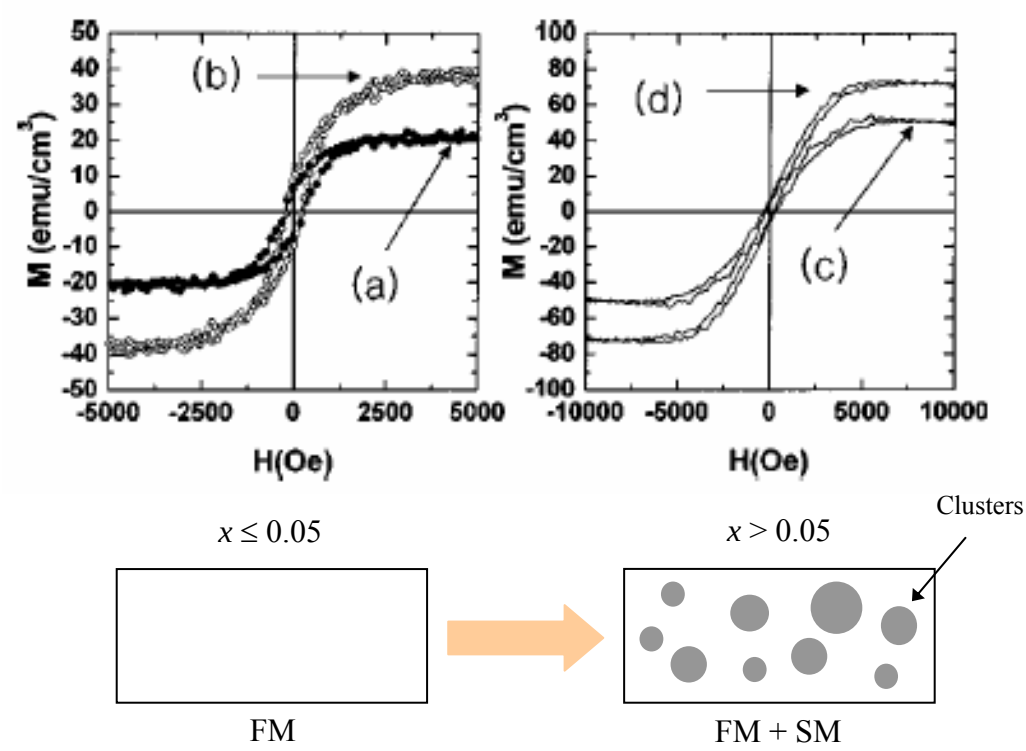


**Figure 2.4** Magnetization hysteresis loops for $Ti_{1-x}Co_xO_2$ thin films with Co contents of $x$=0.03 (a), $x$=0.05 (b), $x$=0.07 (c), $x$=0.12 (d). Plots (a), (b): films with no Co clusters; plots (c), (d): films with Co clusters. Scheme bellow: microstructural model representing the influence of Co content on the magnetic properties of $Ti_{1-x}Co_xO_2$ thin films. FM stands for ferromagnetic and SM for soft magnetic behaviour. Adapted from ref. 47.

Concerning the transport properties of Co-doped $TiO_2$ films, the RT resistivity reported by Matsumoto *et al.*[17] is between 0.1 and 1 Ω cm for films with $x$ = 0.06 deposited on $LaAlO_3$ substrates while the corresponding values measured by Stampe *et al.*[43] are about 6 times larger for 7% Co:$TiO_2$ films grown on the same substrate material. These latter authors studied the resistivity as a function of temperature for two films of different thickness (200 and 1200 nm) grown on $LaAlO_3$ substrate. They showed that the thicker film displays a small resistivity minimum at ~150 K, while the resistivity for the thinner film (200 nm)

increases monotonically with decreasing temperature (figure 2.5). This was found to be a general feature, although there was no definitive "crossover" thickness for which the resistivity changed its behaviour.

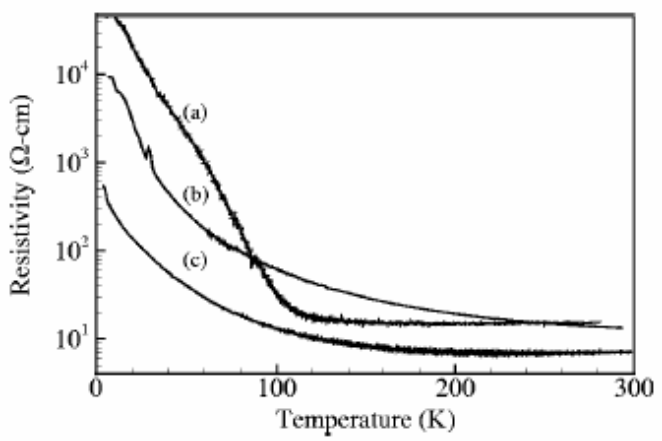


**Figure 2.5** The temperature dependence of the resistivity for: (a) a 600 nm thick undoped $TiO_2$ film, (b) a 200 nm thick 7% Co:$TiO_2$ film, and (c) a 1200 nm thick 7% Co:$TiO_2$ film (from ref. 43).

Hall measurements show *n*-type conduction with estimated carrier concentration of ~$1.4\times10^{18}$ $cm^{-3}$ for undoped $TiO_2$ films and ~$2.1\times10^{18}$ $cm^{-3}$ for $Ti_{0.99}$ $Co_{0.01}O_{2-\delta}$ at 300 K[40]. Matsumoto *et al.*[17] found a carrier concentration of ~$10^{18}$ $cm^{-3}$ which is, according to the authors, scarcely dependent on the Co doping level. Films of anatase $Ti_{1-x}Co_xO_2$, with $0\leq x\leq0.10$, epitaxially grown on $LaSrAlO_4$ (001) substrates by PLD were reported as displaying insulator, semiconductor ($n \sim 1\times10^{17}$ $cm^{-3}$) or metallic (degenerated semiconductor) ($n \sim 2\times10^{19}$ $cm^{-3}$) behaviour, depending on the oxygen pressure used during the growth process[42]. Lower oxygen pressures favour the conductivity, the metallic regime being obtained for a $Ti_{0.97}$ $Co_{0.03}O_2$ grown at $P_{O_2} = 5\times10^{-7}$ Torr.

The effect of magnetic contribution of Co to transport is evidenced more clearly in the low-temperature magnetoresistance (MR) data. MR is defined as $[\rho(H)-\rho(0)]/\rho(0)$ where $\rho(H)$ and $\rho(0)$ are the resistivity values with and without applied magnetic field, respectively. According to Shinde *et al.*[40], the MR is positive and is significant only at very low temperatures which correspond to conditions representing partial ionization of shallow donor states, generally attributed to oxygen vacancies. As can be seen in figure 2.7, the magnetoresistance shows an approximately quadratic dependence on applied field. While the MR at 3 K is about 6% in a field of 8 T for an undoped film, its value increases up to 23% for the $Ti_{0.99}Co_{0.01}O_{2-\delta}$ film and to 40% for the $Ti_{0.98}Co_{0.02}O_{2-\delta}$ one, under comparable conditions. For higher Co concentration, the MR shows saturation due to Co clustering.

Based on the understanding that the oxygen vacancy related states lie close to the bottom of the conduction band, the observed large low temperature positive MR in the $Ti_{0.99}Co_{0.01}O_{2-\delta}$ film can be attributed to Zeeman splitting of this band of states through their coupling to Co spin. Since the lower split band will be occupied the MR should be positive, as experimentally observed. This feature also highlights the significance of the combined role of the magnetic atom and a defect state (vacancy) in controlling the physical and possibly the magnetic properties. Matsumoto *et al.*[17] have reported a similar positive MR value of 60% at 2 K for a $Ti_{0.93}Co_{0.07}O_2$ film under a field of 8 T applied perpendicular to the surface.

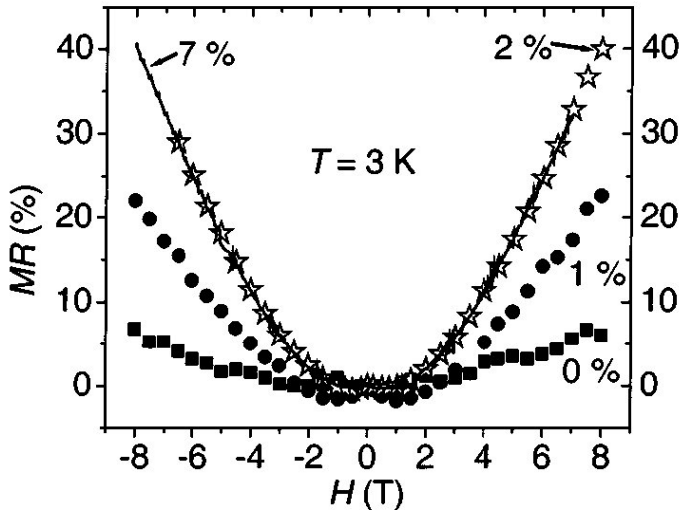


**Figure 2.6** Magnetoresistance as a function of magnetic field for undoped $TiO_2$ and $Ti_{1-x}Co_xO_{2-\delta}$ films (from ref. 40).

## 2.2.3 Origin of ferromagnetism in Co-doped $TiO_2$

As referred above, there is no currently consensus on the origin of ferromagnetism in oxide-based DMS materials, in particular, whether it is an extrinsic effect due to direct interaction between the local moments in magnetic impurity clusters or is indeed an intrinsic property caused by exchange coupling between the spin of the carriers and the local magnetic moments[71]. This is a key issue because spintronics requires polarized charge carriers and this would only be guaranteed if ferromagnetism is intrinsic. Experimental evidence for carrier mediated ferromagnetism in oxide-based DMS is not yet conclusive. In Co:$TiO_2$ rutile phase system, anomalous Hall effect* (AHE)[53,71] and electric

* In ferromagnetic materials the Hall resistivity, $R_{xy}$, includes an additional contribution, known as the

field induced modulation of magnetization by as much as 13.5% have been observed[71,72], arguing for carrier-mediated ferromagnetism. However, AHE was also measured in a sample with magnetic Co clusters, casting doubts about the conclusions that can be drawn from AHE data[67,71].

Recently, theoretical models have been proposed that the ferromagnetism is strongly dependent on the creation and distribution of oxygen vacancies in the Co-doped $TiO_2$ lattice[73]. When the oxygen content of the unit cell is increased, ferromagnetism is suppressed. This seems to support the percolation model of bond magnetic polarons (BMP) developed in 2002 by Kaminski and Das Sarma[74] for $Mn_xGa_{1-x}As$ and specifically applied by Coey *et al*.[23] to magnetically doped oxides†. In short, for the $TiO_2$ crystal, in the event of an oxygen vacancy, the electrons that would be given to the oxygen by the surrounding titanium atoms have no atom to call their own. They become loosely bound to the oxygen vacancy site in what can be considered a hydrogen-like orbital. This constitutes a polaron.

Consider now the interaction of the magnetic cations with the hydrogenic electrons in the impurity band. The donors tend to form BMPs, coupling the 3d moments of the ions within their orbits. The basic idea is illustrated in figure 2.7. Depending on whether the cation 3d orbital is less than half full, or half full or more, the coupling between the cation and the donor electron is ferromagnetic or antiferromagnetic, respectively. Either way, the coupling between two similar impurities within the same donor orbital is ferromagnetic. The polaron radius is a function of the host material's dielectric constant and electron effective mass. If the polaron concentration in the material is large enough to achieve percolation, an entire network of polarons and magnetic cations become interconnected and we observe macroscopic ferromagnetic behaviour.

---

anomalous Hall effect (AHE) which depends directly on the magnetization of the material rather than the applied magnetic field. Therefore, it can be written for these materials that $R_{xy} = r_0 H + r_a M$, where $H$ stands for the applied magnetic filed, $M$ is the magnetization of the sample, and $r_0$ and $r_a$ are constants that characterize the strength of the standard and the anomalous Hall resistivities, respectively. The supplementary $r_a M$ contribution is often much larger than the ordinary Hall effect.

Although a well-recognized phenomenon, there is still debate about its origin in the various materials. The AHE can be either an extrinsic (disorder-related) effect due to spin-dependent scattering of the charge carriers, or an *intrinsic* effect which can be described in terms of the Berry phase effect in the crystal momentum space (see *e.g.* N.A. Sinitsyn, *"Semiclassical Theories of the Anomalous Hall Effect"*, J. Phys. Cond. Matter 20 (2008) 023201)

† The double exchange mechanism by which ferromagnetic order can be explained in manganites[74] gives, at the low carrier density of magnetic oxides, a $T_c$ proportional to the carrier density; therefore, Curie temperatures exceeding room temperature are essentially impossible within the scope of this model.

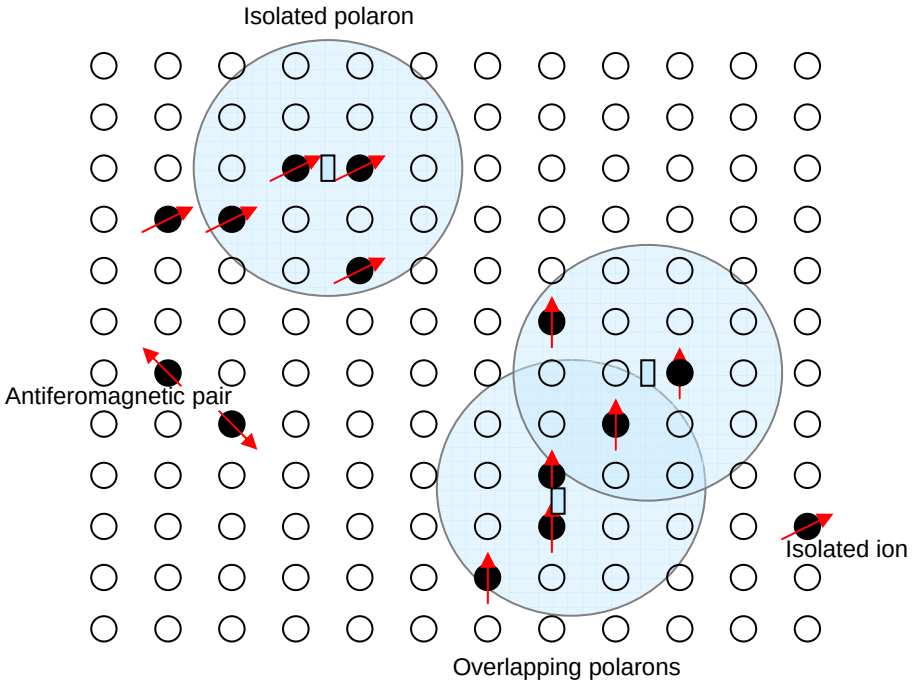


**Figure 2.7** Polaron percolation model as illustrated by Coey *et al.*[23].

More recently, Calderón and Das Sarma[71] have theoretically argued that only a complementary combination of the percolation of magnetic polarons mechanism at lower temperature and the indirect exchange Ruderman–Kittel–Kasuya–Yosida (RKKY) mechanism at higher temperature might explain the high Curie temperatures measured in claimed intrinsic oxide-based DMS, in particular in the Co:$TiO_2$ system for which some experimental evidence for carrier mediated ferromagnetism exists as pointed out above. The theoretical framework of this hybrid model is beyond the scope of this thesis, its details and arguments being described in reference[71].

### 2.2.4 Other transition metal dopants in $TiO_2$

Besides Co doping, there are reports of RT ferromagnetism by doping titanium dioxide with other transition metals such V, Cr, Fe and Ni. Here we briefly resume results published in literature.

Hong *et al.*[60] saw a decreasing trend in the magnetization of their doped anatase $TiO_2$ films with V, Cr, Fe, Co and Ni, deposited on $LaAlO_3$ by PLD. For films prepared at 650 ºC,

V:$TiO_2$ films exhibit a saturation magnetization of 4.23 $\mu_B$/V at RT, the $M_s$ reducing to about one half of this value in the case of Cr doping and rising up again slightly from Fe to Ni dopants. However, this trend is inconsistent with the results of another study carried out by Hong *et al.*[63] during which they found $M_s$ values ranging from 1.3 to 2.7 $\mu_B$/Ni for Ni:$TiO_2$ films and 0.14 $\mu_B$/Fe to Fe:$TiO_2$ films deposited under similar conditions.

Kim *et al.*[75] grew epitaxial Fe-doped $TiO_2$ rutile on $TiO_2$ (110) substrates by OPA-MBE and observed RT ferromagnetism which was associated with the formation of a secondary phase − $Fe_3O_4$, rather than due to a true diluted magnetic oxide semiconductor.

The magnetic moments determined for Fe substituting for Ti in rutile or anatase $TiO_2$ range from 0.14[63] to 2.4 $\mu_B$/Fe[76] suggesting different spin states in the different samples. No relationship between host crystal structure and the magnetic moment was established.

Nguyen *et al.*[77] grew Fe and Ni doped $TiO_2$ rutile thin films by laser ablation on silicon substrates. They reported on Fe and Ni clusters localized mostly near the surface of the films. Fe clusters have been reported also by Kim *et al.*[78].

Cr as dopant in $TiO_2$ was used by different authors. N.H. Hong and co-authors[58] prepared 270 nm thick $Ti_{0.95}Cr_{0.05}O_2$ films on $LaAlO_3$ (001) substrate by PLD method. The maximum saturation magnetic moment achieved in their films was 2.6 $\mu_B$/Cr. Magnetic force microscopy measurements confirmed the RT ferromagnetic order, also ensuring that the Cr-doped $TiO_2$ films certainly have a diluted magnetic structure with the ferromagnetism originated from the doped matrix rather than any type of magnetic cluster.

Droubay *et al.*[59] found that epitaxial Cr-doped $TiO_2$ anatase films grown on $LaAlO_3$ (001) substrates by OPA-MBE are consistently insulating and ferromagnetic at RT, with saturation magnetization of $0.6 \pm 0.05$ $\mu_B$/Cr and coercive field of ~100 Oe. Chromium (III) was found to substitute for Ti in the lattice, with uniform distribution throughout the doped region of the film. Wang *et al.*[79] found that their Cr-doped reduced rutile $TiO_2$ films are ferromagnetic semiconductors up to 400 K. The saturation magnetization of Cr:$TiO_2$ films decreases with increasing Cr doping from 2.9 $\mu_B$/Cr at $x = 0.06$ to 0.9 $\mu_B$/Cr at $x = 0.12$. They also reported that film's resistivity increases with increasing Cr content and with decreasing temperature (semiconductor behaviour).

## 2.3 References


1. C. Chappert, A. Fert and F. N. van Dau, "The emergence of spin electronics in data storage", Nature Mat. 6 (2007) 813-823, and references therein.
2. T. Bland, K. Lee and S. Steinmuller, "The spintronics challenge", Physics World 21 (2008) 24-28, and references therein.
3. D. D. Awschalom and M. E. Flatté, "Challenges for semiconductor spintronics", Nature Phys. 3 (2007) 153-159, and references therein.
4. S. A. Wolf, D. D. Awschalom, R. A. Buhrman, J. M. Daughton, S. von Molnár, M. L. Roukes, A. Y. Chtchelkanova and D. M. Treger, "Spintronics: a spin-based electronics vision for the future", Science 294 (2001) 1488-1495.
5. "125 big questions that face scientific inquiry over the next quarter-century", commemorative issue celebrating the 125th anniversary of the Science Magazine, Science 309 (2005) 82.
6. S. A. Chambers, T. C. Droubay, C. M. Wang, K. M. Rosso, S. M. Heald, D. A. Schwartz, K. R. Kittilstved and D. R. Gamelin, "Ferromagnetism in oxide semiconductors", Materials Today 9 (2006) 28.
7. R. Janisch, P. Gopal and N. A. Spalding, "Transition metal-doped $TiO_2$ and ZnO – present status of the field", J. Phys.: Condens. Matter 17 (2005) R657, and references therein.
8. J. K. Furdyna, "Diluted magnetic semiconductors", J. Appl. Phys. 64 (1988) R29.
9. D. Ferrand, J. Cibert, A. Wasiela, C. Bourgognon, S. Tatarenko, G. Fishman, T. T. Andrearczyk, J. Jaroszynski, S. Kolesnik, T. Dietl, B. Barbara and D. Dufeu, "Carrier-induced ferromagnetism in p-$Zn_{1-x}Mn_xTe$", Phys. Rev. B 63 (2001) 085201.
10. H. Munekata, H. Ohno, S. von Molnar, A. Segmaller, L. L. Chang and L. Esaki, "Diluted magnetic III-V semiconductors", Phys. Rev. Lett. 63 (1989) 1849.
11. H. Ohno, H. Munekata, T. Penney, S. von Molnar and L. L. Chang, "Magnetotransport properties of p-type (In,Mn)As diluted magnetic III-V semiconductors", Phys. Rev. Lett. 68 (1992) 2664.
12. H. Ohno, A. Shen, F. Matsukura, A. Oiwa, A. Endo, S. Katsumoto and Y. Iye, "(Ga,Mn)As: A new diluted magnetic semiconductor based on GaAs", Appl. Phys. Lett. 69 (1996) 363.
13. T. Jungwirth, J. Sinova, J. Masek, J. Kucera and A. H. MacDonald, "Theory of ferromagnetic (III,Mn)V semiconductors", Rev. Mod. Phys. 78 (2006) 809.
14. K. W. Edmonds, K. Y. Wang, R. P. Campion, A. C. Neumann, N. R. S. Farley, B. L. Gallagher and C. T. Foxon, "High-Curie-temperature $Ga_{1-x}Mn_xAs$ obtained by

resistance-monitored annealing", Appl. Phys. Lett. 81 (2002) 4991.

15. D. Chiba, K. Takamura, F. Matsukura and H. Ohno, "Effect of low-temperature annealing on (Ga,Mn)As trilayer structures", Appl. Phys. Lett. 82 (2003) 3020.
16. T. Fukumura, Z. Jin, A. Ohtomo, H. Koinuma and M. Kawasaki, "An oxide-diluted magnetic semiconductor: Mn-doped ZnO", J. Appl. Phys. 75 (1999) 3366.
17. Y. J. Matsumoto, M. Murakami, T. J. Shono, T. Hasegawa, T. Fukumura, M. Kawasaki, P. Ahmet, T. Chikyow, S. Y. Koshihara and H. Koinuma, "Room-temperature ferromagnetism in transparent transition metal-doped titanium dioxide", Science 291 (2001) 854-856.
18. Y. Matsumoto, R. Takahashi, M. Murakami, T. Koida, X.-J. Fan, T. Hasegawa, T. Fukumura, M. Kawasaki, S.-Y. Koshihara and H. Koinuma, "Ferromagnetism in Co-doped $TiO_2$ rutile thin films grown by laser molecular beam epitaxy", Jpn. J. Appl. Phys. 40 (2001) L1204.
19. K. Ueda, H. Tabata and T. Kawai, "Magnetic and electric properties of transition-metal-doped ZnO films", Appl. Phys. Lett. 79 (2001) 988.
20. S. B. Ogale, R. J. Choudhary, J. P. Buban, S. E. Lofland, S. R. Shinde, S. N. Kale, V. N. Kulkarni, J. Higgins, C. Lanci, J. R. Simpson, N. D. Browning, S. Das Sarma, H. D. Drew, R. L. Greene and T. Venkatesan, "High temperature ferromagnetism with a giant magnetic moment in transparent Co-doped $SnO_{2-\delta}$", Phys. Rev. Lett. 91 (2003) 077205.
21. S. N. Kale, S. B. Ogale, and S. R. Shinde, M. Sahasrabuddhe, V. N. Kulkarni, R. L. Greene and T. Venkatesan, "Magnetism in cobalt-doped $Cu_2O$ thin films without and with Al, V, or Zn codopants", Appl. Phys. Lett. 82 (2003) 2100.
22. J. Philip, N. Theodoropolou, G. Berera, J. S. Moodera and B. Satpati, "High-temperature ferromagnetism in manganese-doped indium-tin oxide films", Appl. Phys. Lett. 85 (2004) 777.
23. J. M. D. Coey, M. Venkatesan and C. B. Fitzgerald, "Donor impurity band exchange in dilute ferromagnetic oxides", Nature Mater. 4 (2005) 173, and references therein.
24. T. Fukumuraa, Y. Yamadaa, H. Toyosakia, T. Hasegawab, H. Koinuma and M. Kawasakia, "Exploration of oxide-based diluted magnetic semiconductors toward transparent spintronics", Appl. Surf. Sci. 223 (2004) 62.
25. A. L. Linsebigler, G. Lu and J. T. Yates, Jr., "Photocatalysis on $TiO_2$ surfaces: principles, mechanisms, and selected results", Chem. Rev. 95 (1995) 735.
26. R. Wang, K. Hashimoto, A. Fujishima, M. Chikuni, E. Kojima, A. Kitamura, M. Shimohigoshi and T. Watanabe, "Light-induced amphiphilic surfaces", Nature 388 (1997) 431.

27. J. Zhuang, C. N. Rusu and T. Yates, Jr., "Adsorption and photooxidation of $CH_3CN$ on $TiO_2$", J. Phys. Chem. B 103 (1999) 6957.

28. V. Gayvoronsky, A. Galas, E. Shepelyavyy, T. H. Dittrich, V. Yu. Timoshenko, S. A. Nepijko, M. S. Brodyn and F. Koch, "Giant nonlinear optical response of nanoporous anatase layers", Appl. Phys. B 80 (2005) 97.

29. M. Grätzel, "Dye-sensitized solar cells", J. Photochem. Photobiol. C: Photochem. Rev. 4 (2003) 145.

30. X. Y. Du, Y. Wang, Y. Y. Mu, L. L. Gui, P. Wang and Y. Q. Tang, "A new highly selective $H_2$ sensor based on $TiO_2$/PtO−Pt dual-layer films", Chem. Mater. 14 (2002) 3953.

31. S. K. Kim, W.-D. Kim, K.-M. Kim, C. S. Hwang and J. Jeong, "High dielectric constant $TiO_2$ thin films on a Ru electrode grown at 250 °C by atomic-layer deposition", J. Appl. Phys. 85 (2004) 4112.

32. U. Diebold, "The surface science of titanium dioxide", Surf. Sci. Rep. 48 (2003) 53.

33. J. Pascual, J. Camassel and M. Mathieu, "Fine structure in the intrinsic absorption edge of $TiO_2$", Phys. Rev. B 18 (1978) 5606.

34. N. Daude, C. Gout and C. Jouanin, "Electronic band structure of titanium dioxide", Phys. Rev. B 15 (1977) 3229.

35. H. Tang, K. Prasad, R. Sanjinès, P.E. Schmid and F. Lévy, "Electric and optical properties of $TiO_2$ anatase thin films", J. Appl. Phys. 75 (1994) 2042.

36. H. Tang, H. Berger, P.E. Schmid, F. Lévy and G. Burri, "Photoluminescence in $TiO_2$ anatase single crystals", Solid State Commun. 87 (1993) 847.

37. T. Toyoda R. Taira, Q. Shen and M. Ohmori, "Photoacustic spectra of mixed TiO2 ultrafine powders with rutile and anatase structures", Jpn. J. Appl. Phys. 40 (2001) 3587.

38. M. Koelscha, S. Cassaignona, J. F. Guillemolesb and J. P. Joliveta, "Comparison of optical and electrochemical properties of anatase and brookite $TiO_2$ synthesized by the sol–gel method", Thin Solid Films 403-404 (2002) 312.

39. T. Fukumura, H. Toyosaki and Y. Yamada, "Magnetic oxide semiconductors", Semicond. Sci. Technol. 20 (2005) S103.

40. S. R. Shinde, S. B. Ogale, S. Das Sarma, J. R. Simpson, and H. D. Drew, S. E. Lofland and C. Lanci, J. P. Buban and N. D. Browning, V. N. Kulkarni, J. Higgins, R. P. Sharma, R. L. Greene and T. Venkatesan, "Ferromagnetism in laser deposited anatase $Ti_{1-x}Co_xO_{2-\delta}$ films", Phys. Rev. B 67 (2003) 115211

41. D. H. Kim, J. S. Yang, K. W. Lee, S. D. Bu, and T. W. Noh, S.-J. Oh, Y.-W. Kim, J.-S. Chung, H. Tanaka, H. Y. Lee and T. Kawai, "Formation of Co nanoclusters in

epitaxial $Ti_{0.96}Co_{0.04}O_2$ thin films and their ferromagnetism", Appl. Phys. Lett. 81 (2002) 2421.

42. Y. Yamada, H. Toyosaki, A. Tsukazaki, T. Fukumura, K. Tamura,Y. Segawa, K. Nakajima, T. Aoyama, T. Chikyow, T .Hasegawa, H. Koinuma and M. Kawasaki, "Epitaxial growth and physical properties of a room temperature ferromagnetic semiconductor: Anatase phase $Ti_{1-x}Co_xO_2$", J. Appl. Phys. 96 (2004) 5097.
43. P. A. Stampe, R. J. Kennedy, Y. Xin and J. S. Parker, "Investigation of the cobalt distribution in $TiO_2$:Co thin films", J. Appl. Phys. 92 (2002) 7114.
44. J. S. Higgins, S. R. Shinde, S. B. Ogale, T. Venkatesan and R. L. Greene, "Hall effect in cobalt-doped $TiO_{2-\delta}$", Phys Rev B 69 (2004) 073201.
45. H. S. Yang, J. Choi, V. Craciun and R. K. Singh, "Ferromagnetism of anatase $Ti_{1-X}Co_xO_{2-\delta}$ films grown by ultraviolet-assisted pulsed laser deposition", J. Appl. Phys. 93 (2003) 7873.
46. W. K. Park, R. J. Ortega-Hertogs and J. S. Moodera, "Semiconducting and ferromagnetic behavior of sputtered Co-doped $TiO_2$ thin films above room temperature", J. Appl. Phys. 91 (2002) 8093.
47. N. J. Seong, S. G. Yoon and C. R. Cho, "Effects of Co-doping level on the microstructural and ferromagnetic properties of liquid-delivery metalorganic-chemical-vapor-deposited $Ti_{1-x}Co_xO_2$ thin films", Appl. Phys. Lett. 81 (2002) 4209.
48. S. A. Chambers, S. Thevuthasan, R. F. C. Farrow, R. F. Marks, J. U. Thiele, L. Folks, M. G. Samant, A. J. Kellock, N. Ruzycki, D. L. Ederer and U. Diebold, "Epitaxial growth and properties of ferromagnetic co-doped $TiO_2$ anatase", Appl. Phys. Lett. 79 (2001) 3467.
49. S. A. Chambers, C. M. Wang, S. Thevuthasan, T. Droubay, D. E. McCready, A. S. Lea, V. Shutthababdan and C. F. Jr Windisch, "Epitaxial growth and properties of MBE-grown ferromagnetic Co-doped $TiO_2$ anatase films on $SrTiO_3(001)$ and $LaAlO_3(001)$", Thin Solid Films 418 (2002) 197.
50. S. A. Chambers, T. Droubay, C. M. Wang, A. S. Lea, R. F. C. Farrow, L. Folks, V. Deline and S. Anders, "Clusters and magnetism in epitaxial Co-doped $TiO_2$ anatase", Appl. Phys. Lett. 82 (2003) 1257.
51. J.-Y. Kim, J.-H. Park, B.-G. Park, H.-J. Noh, S.-J. Oh, J. S. Yang, D.-H. Kim, S. D. Bu, T.-W. Noh, H.-J. Lin, H.-H. Hsieh, and C. T. Chen, "Ferromagnetism induced by clustered Co in Co-doped anatase $TiO_2$ thin films", Phys. Rev. Lett. 90 (2003) 017401.
52. M. Murakami, Y. Matsumoto, T. Hasegawa, P. Ahmet, K. Nakajima, T. Chikyow, H. Ofuchi, I. Nakai and H. Koinuma, "Cobalt valence states and origins of ferromagnetism in Co doped $TiO_2$ rutile thin films", J. Appl. Phys. 95 (2004) 5330.

53. H. Toyosaki, T. Fukumura, Y. Yamada, K. Nakajima, T. Chikyow, T. Hasegawa, H. Koinuma and M. Kawasaki, "Anomalous Hall effect governed by electron doping in a room-temperature transparent ferromagnetic semiconductor", Nature Mat. 3 (2004) 221.

54. Y. L. Soo, G. Kioseoglou, S. Kim, Y. H. Kao, D. P. Sujatha, J. Parise, R. J. Gambino and P. I. Gouma, "Local environment surrounding magnetic impurity atoms in a structural phase transition of Co-doped $TiO_2$ nanocrystal ferromagnetic semiconductors", Appl.Phys. Lett. 81 (2002) 655.

55. N. H. Hong, W. Prellier, J. Sakai and A. Ruyter, "Substrate effects on the room-temperature ferromagnetism in Co-doped $TiO_2$ thin films grown by pulsed laser deposition", J. Appl. Phys. 95 (2004) 7378.

56. M. L. Cui, J. Zhu, X. Y. Zhong, Y. G. Zhao and X. F. Duan, "Cobalt valence in epitaxial $Ti_{0.93}Co_{0.07}O_2$ anatase", Appl. Phys. Lett. 85 (2004) 1698.

57. N. H. Hong, J. Sakai, W. Prellier and A. Ruyter, "Room temperature ferromagnetism in anatase $Ti_{0.95}V_{0.05}O_2$ thin films", Physica B: Cond. Matt. 355 (2005) 295.

58. N. H. Hong, A. Ruyter, W. Prellier and J. Sakai, "Room temperature ferromagnetism in anatase $Ti_{0.95}Cr_{0.05}O_2$ thin films: Clusters or not?", Appl. Phys. Lett. 85 (2004) 6212.

59. T. Droubay, S. M. Heald, V. Shutthanandan, S. Thevuthasan, S. A. Chambers andJ. Osterwalder, "Cr-doped $TiO_2$ anatase: A ferromagnetic insulator", J. Appl. Phys. 97 (2005) 046103.

60. N. H. Hong, J. Sakai, W. Prellier, A. Hassini, A. Ruyter and F. Gervais, "Ferromagnetism in transition-metal-doped $TiO_2$ thin films", Phys. Rev. B 70 (2004) 195204.

61. D. H. Kim, J. S. Yang, Y. S. Kim, Y. J. Chang, T.W. Noh, S.D. Bu, Y.-W. Kim, Y.D. Park, S. J. Pearton and J. -H. Park, "Superparamagnetism in Co ion-implanted epitaxial anatase $TiO_2$ thin films", Ann. Phys. 13 (2004) 70.

62. D. H. Kim, J. S. Yang, Y. S. Kim, T. W. Noh, S. D. Bu, S.-I. Baik, Y.-W. Kim, Y. D. Park, S. J. Pearton, J.-Y. Kim, J.-H. Park, H.-J. Lin, C. T. Chen and Y. J. Song, "Effects of high-temperature postannealing on magnetic properties of Co-doped anatase $TiO_2$ thin films", Phys. Rev. B 71 (2005) 014440.

63. N. H. Hong, W. Prellier, J. Sakai and A. Hassini, "Fe- and Ni-doped $TiO_2$ thin films grown on $LaAlO_3$ and $SrTiO_3$ substrates by laser ablation", Appl. Phys. Lett. 84 (2004) 2850.

64. H. S. Yang and R. K. Singh, "Growth and properties of Co-doped $TiO_2$ thin films grown on buffered Si substrate", J. Appl. Phys. 95 (2004) 7192.

65. M. Murakami, Y. Matsumoto, K. Nakajima, T. Makino, Y. Segawa, T. Chikyow, P.

Ahmet, M. Kawasaki and H. Koinuma, "Anatase $TiO_2$ thin films grown on lattice-matched $LaAlO_3$ substrate by laser molecular-beam epitaxy", Appl. Phys. Lett. 78 (2001) 2664.

66. G. C. Han, P. Luo, Z. B. Guo, F. U. Nahar, M. Tay, Y. H. Wu and S. J. Wang, "Co-doped $TiO_2$ epitaxial thin films grown by sputtering", Thin Solid Films 505 (2006) 137.

67. S. R. Shinde, S. B. Ogale, J. S. Higgins, H. Zheng, A.J. Millis, V.N. Kulkarni, R. Ramesh, R.L. Greene and T. Venkatesan, "Co-occurrence of superparamagnetism and anomalous Hall effect in highly reduced Cobalt-doped rutile $TiO_{2-\delta}$ films", Phys. Rev. Lett. 92 (2004) 166601.

68. J. M. D. Coey, "Dilute magnetic oxides", Current Opinion in Solid State and Materials Science 10 (2006) 86, and references therein.

69. F. Golmar, A. M. M. Navarro, C. E. R. Torres, F. H. Sánchez, F. D. Saccone, P. C. S. Claro, G. A. Benítez and P. L. Schilardi, "Extrinsic origin of ferromagnetism in single crystalline LaAlO3 substrates and oxide films", Appl. Phys. Lett. 92 (2008) 262503.

70. H. Weng, X. Yang, J. Dong, H. Mizuseki, M. Kawasaki and Y. Kawazoe, "Electronic structure and optical properties of the Co-doped anatase $TiO_2$ studied from first principles", Phys. Rev. B 69 (2004) 125219.

71. M. J. Calderón and S. Das Sarma, "Theory of carrier mediated ferromagnetism in dilute magnetic oxides", Annals of Physics 322 (2007) 2618.

72. T. Zhao, S.R. Shinde, S.B. Ogale, H. Zheng, T. Venkatesan, R. Ramesh and S. Das Sarma, "Electric field effect in diluted magnetic insulator anatase Co:□□$TiO_2$", Phys. Rev. Lett. 94 (2005) 126601.

73. J.E. Jaffe, T.C. Drouban and S.A. Chambers, "Oxygen vacancies and ferromagnetism in $Co_xTi_{1-x}O_{2-x-y}$", J. Appl. Phys. 97 (2005) 073908.

74. A. Kaminski and S. Das Sarma, "Polaron percolation in diluted magnetic semiconductors", Phys. Rev. Lett. 88 (2002) 247202.

75. Y. J. Kim, S. Thevuthasan, T. Droubay, A. S. Lea, C. M. Wang, V. Shutthanandan, S. A. Chambers, R. P. Sears, B. Taylor and B. Sinkovic, "Growth and properties of molecular beam epitaxially grown ferromagnetic Fe-doped $TiO_2$ rutile films on $TiO_2$(110)", Appl. Phys. Lett. 84 (2004) 3531.

76. Z. Wang, W. Wang, J. Tang, L. D. Tung, L. Spinu and W. Zhou, "Extraordinary Hall effect and ferromagnetism in Fe-doped reduced rutile", Appl. Phys. Lett. 83 (2003) 518.

77. N. H. Honga, J. Sakaib and W. Prellier, "Distribution of dopant in Fe:$TiO_2$ and Ni:$TiO_2$ thin films", J. Magn. and Mag. Mat. 281 (2004) 347.

78. E. C. Kim, S. H. Moon, S. I. Woo, J. H. Cho, Y. Gu. Joh and D. H. Kim, "Mössbauer study and magnetic properties of $Ti_{0.99}{}^{57}Fe_{0.01}O_2$", Sol. Stat. Commun. 132 (2004) 477.

79. Z. Wang, J. Tang, H. Zhang, V. Golub, L. Spinu and L. D. Tung, "Ferromagnetism in chromium-doped reduced-rutile titanium dioxide thin films", J. Appl. Phys. 95 (2004) 7381.